Self-consistent medium polarization in spin-polarized ^{3}He

W. H. Dickhoff
Department of Physics, Washington University, St. Louis, Missouri 63130

H. Müther
Institut für Theoretische Physik, Universität Tübingen, D-7400 Tübingen, Federal Republic of Germany

A. Polls
Departament de Fisica Teorica, Universitat de Barcelona, 08028-Barcelona, Spain
(Received 23 March 1987)

A microscopic calculation of the residual particle-hole (p-h) interaction in spin-polarized ^{3}He is performed. As a starting point the Brueckner G matrix is used which is supplemented by including the phonon exchange terms self-consistently. An important ingredient in this microscopic version of the induced interaction is the treatment of the full momentum dependence of the interaction. This allows a consistent description of the Landau limit (Pauli-principle sum rule for the Landau parameters is fulfilled) but also enables a detailed study of the p-h interaction at finite momentum transfers. A comparison with correlated basis functions results shows good agreement for momentum transfers larger than the Fermi momentum.

I. INTRODUCTION

Surveying the recent literature, one may conclude that substantial progress has been made in obtaining samples of highly polarized liquid ^{3}He. The original suggestion of Castaing and Nozières[1] was the rapid melting of highly polarized solid ^{3}He. The most recent experiments have already resulted in polarizations of 55% (Ref. 2) and 65% (Ref. 3). Other experimental routes are also being explored.[4] Beside these experimental activities, there is also an expanding literature of theoretical work on purely polarized ^{3}He. The first suggestions on polarized liquid ^{3}He were in fact theoretical.[5] The equilibrium properties of ^{3}He↑ have been studied in a variety of approaches. Variational calculations of the binding energy indicated that the polarized phase would be more bound than the normal phase.[6,7] This proved only that it is more difficult to describe the normal phase accurately. More recent variational calculations either including spin-dependent correlations[8,9] or including triplet correlations and backflow,[10] have reversed tihs situation again. In Ref. 6 and 10 it is shown that three-body and state-dependent correlations give a substantial contribution to the binding energy of the normal liquid, whereas they are less important for the fully polarized system.

The conclusion that the fully polarized system is theoretically easier to handle, was also derived from a different point of view in Ref. 11, where the Landau parameters for ^{3}He↑ were calculated with the method of Ref. 12. In this semimicroscopic approach this was shown to be due to the "freezing out" of the spin fluctuations. The residual particle-hole interaction is calculated with special emphasis on the induced one-phonon exchange terms, the so-called induced interaction,[13] which is also considered in this paper.

From yet another method, which uses the Galitskiĭ-Feynman T-matrix approach, similar results have been obtained for the fully polarized liquid,[14] although this method strongly overbinds the normal system and is probably not very accurate in this case.[15] With this method it is possible to go beyond the Landau limit and study the dynamic structure function of the system as is done in Ref. 16. This current interest in calculating the excitations of the system instead of restricting oneself to the binding energy, can be rephrased in an interest in the particle-hole interaction (also at finite momentum transfer q) which determines the nature of these excitations and the amount of collectivity they carry. In a recent study[17] within the method of correlated basis functions (CBF) this particle-hole interaction has been calculated in the local approximation.[18]

In the present paper an attempt is made to calculate the residual particle-hole interaction with a method which has its roots in perturbation theory. It presents a microscopic calculation of the induced interaction starting from the bare atom-atom interaction which is taken from Ref. 19. The philosophy behind this calculation is to start with a residual interaction which takes into account the important short-range repulsion between the atoms. Such an interaction should be well represented by a G matrix. In a next step one asks the question: Can this residual interaction lead to strong collective effects? To answer this question, one then solves a random-phase-approximation (RPA) type integral equation for different values of the momentum transfer q. The RPA equation is solved in the static case (excitation energy $\omega=0$); this allows the study of the stability of the normal ground state with respect to particle-hole excitations as a function of q. It is useful to introduce stability functions which can be viewed as a generalization of the

stability conditions[20] on the Landau parameters at $q=0$ to finite q. In the case of a repulsive particle-hole (p-h) interaction a possible zero-sound mode can be sustained which is pushed up in energy out of the normal p-h continuum. In this case the stability conditions are automatically fulfilled at $\omega=0$. For an attractive p-h interaction of sufficient strength, however, it is possible to violate the stability condition.

Before reaching the conclusion that the chosen ground state is indeed unstable, one should keep in mind that the residual interaction which was used to reach such a conclusion does not contain important contributions which tend to prevent this instability. Such a contribution is represented by the exchange of this "unstable" collective mode between the particle and the hole, as shown in Fig. 1. This term is not included in the G matrix and it is highly plausible that one must include such terms if one wants to study collective effects microscopically. Indeed the original divergence will be canceled by the diverging exchange term of Fig. 1, which in turn should be calculated with the proper cancellation effect included and so on. Obviously this leads to a self-consistency problem for the residual p-h interaction. This is a microscopic version of the induced interaction.[13]

It is a well-known fact that normal ^{3}He is extremely difficult to describe microscopically. Only recently, Monte Carlo techniques are reported to give accurate values for the binding energy of the ground state.[21] For this reason and also because other methods[8-11,14] lead to the conclusion that the fully polarized liquid is more amenable to a theoretical description, we will consider this system in this paper.

Although the spin fluctuation degree of freedom is "frozen out", resulting in a simplification of the theoretical description, one must expect it to be highly sensitive to the treatment of the Pauli principle. Whereas, for example, the spin isospin degeneracy in nuclear matter leads to exchange terms which are roughly a factor $\frac{1}{4}$ of the direct terms (at least for a spin isospin independent interaction), this factor is already $\frac{1}{2}$ for normal ^{3}He. It is, however, 1 for the fully polarized liquid. This explains why a careful treatment of exchange terms as, e.g., depicted in Fig. 1,is expected to be important. This issue becomes even more urgent when one observes coherence in summing the RPA series with the G matrix as the residual p-h interaction. In this case the higher-order screening contributions in Fig. 1 will also acquire some importance and the full self-consistent treatment of the residual p-h interaction is required.

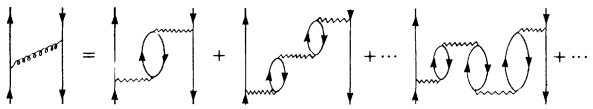

FIG. 1. Phonon exchange term which contributes to the residual p-h interaction. The wavy lines on the right-hand side depict the Brueckner G matrix.

Since the dominant relative motion of the ^{3}He atoms is of P-wave nature in ^{3}He↑, again due to the Pauli principle, one must expect a considerable momentum dependence of the residual interaction. This in turn implies that it is crucial to treat the full momentum transfer q dependence, since results[10] obtained in the Landau limit $q=0$ may not be representative for the calculation of the full induced interaction. Another advantage in the calculation of the induced interaction is that the Pauli principle sum rules for the Landau parameters[22] are, in principle, automatically fulfilled. In the light of the above discussion on the relevance of exchange effects this is an important advantage.

Another consequence of the enhanced importance of the Pauli principle is the increased sensitivity to the nonlocality due to the exchange contributions. Indeed the strong momentum dependence of the interaction which makes it necessary to study the p-h interaction at finite q implies that one can expect a similar necessity to treat the full momentum dependence in the exchange channel. In this paper we therefore employ a method to solve the RPA integral equation which allows the treatment of the full momentum dependence of the p-h interaction.[23]

The paper is organized as follows. In Sec. II we briefly discuss the calculation of the G matrix and give a more-detailed discussion of the calculation of the induced interaction. Also, the analysis of the results for the p-h propagator are discussed which lead to the introduction of stability functions as well as a clean definition of an effective q-dependent p-h interaction, which in principle can be compared to the polarization potential approach[24,25] and the results of Ref. 17. Section III contains the results for the Landau parameters and the p-h interaction at finite momentum transfer q. Finally, a summary and some conclusions are given in Sec. IV.

II. MICROSCOPIC CALCULATION OF THE INDUCED INTERACTION

In this section we discuss the formalism and the calculational scheme to arrive at the induced interaction starting from the bare atom-atom interaction. In Sec. II A we will first introduce the calculation of the G matrix which turns the bare potential into a well-behaved effective interaction. At this point it is also useful to introduce the particle-hole transformation which is necessary to change from the particle-particle channel in which the G matrix is calculated, to the particle-hole channel in which the RPA equation is formulated. The Landau limit of the p-h interaction and the Landau parameters are also discussed at this point. Section II B will then be devoted to a discussion of the RPA equation and the way in which it is solved. It is also shown here, how one can construct the contribution to the induced interaction and the steps one has to take until self-consistency is achieved. The analysis of the induced interaction in terms of stability functions and q-dependent effective interactions is introduced in Sec. II C.

A. Calculation of the G matrix

As discussed in the Introduction, we will use as a starting point for the residual p-h interaction the Brueckner G matrix. Since the purpose of this paper is a microscopic study of the p-h interaction as a function of the momentum transfer q, we will confine ourselves to a calculation of the G matrix in the standard fashion.[26] This means that the single-particle (SP) spectrum is calculated self-consistently from the on-shell precription

$$\varepsilon(k)=\frac{k^2}{2m}+\sum_{k'<k_F}\langle kk'\,|\,G(\varepsilon(k)+\varepsilon(k'))\,|\,kk'\rangle \tag{2.1}$$

for momenta $k<k_F$ and no insertions are made into particle lines. For momenta below k_F this SP spectrum can be approximated quite accurately by an effective-mass spectrum

$$\varepsilon(k)=\frac{k^2}{2m_B^*}+U_0\ , \tag{2.2}$$

where m_B^* and U_0 are determined by calculating $\varepsilon(k)$ for two values of k below k_F. It has been emphasized in the literature[27,28] that this choice for the SP potential leads to a substantial reduction of the total effective mass in the case of nuclear matter. In addition, one should use a continuous SP spectrum across k_F if one is interested in p-h related quantities, as we are here. Although our calculation does not include the enhancement of the effective mass at the Fermi surface, this might not be such a serious problem since the results of Ref. 17, which include the E mass, do not show this enhancement for ^{3}He↑, and in Ref. 11 it was also found that the effective mass at k_F has a value <1. One should, however, note that an enhancement for the effective mass in ^{3}He↑ due to the E mass is observed in Ref. 14 as noted in Ref. 28. Concerning the choice of the SP spectrum in p-h calculations, we have chosen the prescription

$$\varepsilon(k)=\frac{k^2}{2m_L^*}+U_0\ , \tag{2.3}$$

where m_L^* is calculated from the Landau parameter F_1 according to

$$\frac{m_L^*}{m}=1+\tfrac{1}{3}F_1\ . \tag{2.4}$$

This prescription is used for all values of k, ensuring the continuity of the SP spectrum. Clearly this choice is not consistent with the calculation of the G matrix where a gap in the spectrum is used; we felt, however, that the more elaborate calculations including a self-consistent SP spectrum according to Eq. (1) would go beyond the main purpose of this paper, i.e., to the study the p-h interaction in more detail.

Some of the results for the binding energy will be shortly discussed in Sec. III. As is the usual case with lowest-order Brueckner theory, one does not obtain a sufficiently attractive contribution to the potential energy as compared to other methods.[8–10,14] For the purpose of the present paper this does not present a serious drawback since the binding energy is an average of the residual interaction. Whether the residual interaction, in this case the G matrix, is slightly too weak should then be put into the perspective of the corrections which are obtained when the induced interaction is added. These contributions turn out to be substantial and certainly larger than the differences between, e.g., the Galitskii-Feynman T matrix and the G matrix.

Before discussing the RPA integral equation in Sec. II B, it is useful to describe shortly the particle-hole transformation which transforms the particle-particle (p-p) channel to the particle-hole (p-h) channel. This transformation involves both the recoupling of the spins as well as a recoupling of the momentum vectors. In the case of nuclear matter this has been discussed in detail in Ref. 23. In the case of ^{3}He↑ this transformation is considerably simplified since each point in k space can only be occupied by one particle and there are no tensor forces present. Schematically, a general p-h transformation can be written as follows:

$$\langle 1;2^{-1}\,|\,V\,|\,3;4^{-1}\rangle_{ph}=\langle 1;\bar{4}\,|\,V\,|\,\bar{2};3\rangle_{pp}\ , \tag{2.5}$$

where the labels 1–4 refer to a complete set of single-particle quantum numbers. The superscript -1 refers to a hole state with corresponding quantum numbers and the overbar represents the time-reversed state. The quantum numbers for ^{3}He↑ are the momentum and the spin projection of the particles. Writing Eq. (2.5) for this situation explicitly, one obtains

$$\langle \mathbf{p}_1,m_1;(\mathbf{p}_2,m_2)^{-1}\,|\,V\,|\,\mathbf{p}_3,m_3;(\mathbf{p}_4,m_4)^{-1}\rangle_{ph}$$
$$=(-1)^{1/2+m_4}\langle \mathbf{p}_1,m_1;-\mathbf{p}_4,-m_4\,|\,V\,|\,-\mathbf{p}_2,-m_2;\mathbf{p}_3,m_3\rangle_{pp}(-1)^{1/2+m_2}\ . \tag{2.6}$$

Without loss of generality all spins are pointing up which is denoted by ↑. This means that all the spins on the right-hand side of Eq. (2.6) point upward, which in turn implies that the corresponding hole states on the left-hand side have their spin pointing downward. It is therefore not possible to couple the spins of a particle and a hole to a good total spin S since only particles with spin ↑ and holes with spin ↓ are available. The p-h states in ^{3}He↑ are therefore a linear combination of states with good total spin

$$|\,\mathbf{p}_1\uparrow;\mathbf{p}_2\downarrow^{-1}\rangle=\frac{1}{\sqrt{2}}\{\,|\,(1,2^{-1})S=0,M_S=0\rangle+|\,(1,2^{-1})S=1,M_S=0\rangle\}\ . \tag{2.7}$$

For p-h calculations, this is the crucial difference with the normal liquid where both channels contribute separately,

the $S=0$ channel corresponding to density waves and the $S=1$ channel corresponding to spin waves.

The p-p matrix elements on the right-hand side of Eq. (2.6) are calculated by solving the Bethe-Goldstone equation in the momentum-space partial-wave representation. The different partial-wave channels can then be combined to get the momentum-space representation which is used in Eq. (2.6). Suppressing the spin quantum numbers in the p-h matrix elements, one finally ends up with the following result:

$$\langle \mathbf{q},\mathbf{p} \mid V \mid \mathbf{q},\mathbf{p}' \rangle_{ph} = \sum_{\text{odd } L} \frac{(2L+1)}{4\pi} \langle \mathbf{K},kLS=1 \mid V \mid \mathbf{K},k'LS=1 \rangle_{pp} P_L(\cos\theta_{\mathbf{k},\mathbf{k}'}) , \tag{2.8}$$

where the momentum variables are defined in the following way:

$$\begin{aligned} \mathbf{q} &= \mathbf{p}_1 - \mathbf{p}_2 = \mathbf{p}_3 - \mathbf{p}_4 , \\ \mathbf{p} &= \tfrac{1}{2}(\mathbf{p}_1 + \mathbf{p}_2) , \\ \mathbf{p}' &= \tfrac{1}{2}(\mathbf{p}_3 + \mathbf{p}_4) . \end{aligned} \tag{2.9}$$

The momentum variable $\mathbf{q}$ corresponds to the total p-h momentum, whereas $\mathbf{p}$ and $\mathbf{p}'$ correspond to the relative momenta of the final and initial p-h state. In a similar way one can relate the corresponding momenta $\mathbf{K}$, $\mathbf{k}$, and $\mathbf{k}'$ in the p-p channel to the momenta of the individual particles

$$\begin{aligned} \mathbf{K} &= \mathbf{p}_1 - \mathbf{p}_4 = \mathbf{p}_3 - \mathbf{p}_2 , \\ \mathbf{k} &= \tfrac{1}{2}(\mathbf{p}_1 + \mathbf{p}_4) , \\ \mathbf{k}' &= -\tfrac{1}{2}(\mathbf{p}_2 + \mathbf{p}_3) . \end{aligned} \tag{2.10}$$

From Eqs. (2.9) and (2.10) one can then easily obtain the relations between the set of p-h momenta $\mathbf{q},\mathbf{p},\mathbf{p}'$ and the set of p-p momenta $\mathbf{K},\mathbf{k},\mathbf{k}'$. It should be noted that the p-p matrix elements on the right-hand side of Eq. (2.8) are antisymmetrized; therefore, those with even orbital angular momentum L vanish.

The limit $q \to 0$ for the p-h matrix elements corresponds to the so-called Landau limit. In the case of the G matrix one furthermore has to specify the energy; in the Landau limit in which also the excitation energy of the system $\omega \to 0$, this energy corresponds to twice the Fermi energy ε_F. In the calculations this choice was also made for momenta $q \neq 0$, see also Ref. 23. Obviously, the p-h matrix elements of the G matrix will only depend on the relative momenta $\mathbf{p}$ and $\mathbf{p}'$ when $q=0$. Since one is interested in p-h propagation only, the only possible p-h states in this limit have the absolute value of the relative momentum equal to k_F. The only remaining variable is then the angle between the incoming and outgoing relative momentum. Denoting this limit of the p-h interaction by $V(\mathbf{p},\mathbf{p}')$ one obtains the so-called Landau parameters as expansion coefficients with respect to the complete set of Legendre polynomials

$$N_0 V(\mathbf{p},\mathbf{p}') = \sum_{l=0}^{\infty} F_l P_l(\cos\theta_{\mathbf{p},\mathbf{p}'}) . \tag{2.11}$$

The Landau parameters F_l are dimensionless since the interaction V is multiplied with the density of states at the Fermi surface

$$N_0 = \frac{m_L^* k_F}{2\pi^2} . \tag{2.12}$$

The effective mass m_L^* was already defined in Eq. (2.4). From the Landau parameter F_0 can deduce the incompressibility

$$\beta = \frac{k_F^2}{3m_L^*}(1+F_0) . \tag{2.13}$$

The Pauli principle sum rule for the fully polarized liquid is finally given by

$$S_P \equiv \sum_{l=0}^{\infty} \frac{F_l}{1+F_l/(2l+1)} = 0 . \tag{2.14}$$

We note that the same antisymmetry requirement leads to

$$S_A \equiv \sum_{l=0}^{\infty} F_l = 0 \tag{2.15}$$

if an antisymmetrized interaction like the G matrix is used to calculate the Landau parameters.

B. Solution of the RPA equation and construction of the induced interaction

In this section we will first introduce the concepts of the induced interation. In a next step the solution of the RPA integral equation is discussed. In fact, to arrive at the induced interaction it will be necessary to solve this linear integral equation until the induced interaction is calculated self-consistently. To make this point more clear, the nonlinear scheme to calculate the induced interaction is depicted in Fig. 2. The starting point in these considerations is the p-h propagator Π, which is obtained by iterating the free p-h propagator $\Pi^{(0)}$ with the irreducible p-h interaction I. For our purposes it is most convenient to consider the two-time formulation as given, e.g., in Ref. 29. This has the advantage that there is only one energy variable involved which corresponds to the excitation energy of the system. For the free p-h propagator one then obtains the result

$$\begin{aligned} \Pi^{(0)}(\mathbf{p};\mathbf{q},\omega) = \int \frac{d\omega'}{2\pi i} & g(\mathbf{p}+\mathbf{q}/2,\omega'+\omega/2) \\ & \times g(\mathbf{p}-\mathbf{q}/2,\omega'-\omega/2) , \end{aligned} \tag{2.16}$$

where g is the SP Green function

$$g(\mathbf{k},E) = \frac{\Theta(|\mathbf{k}|-k_F)}{E-\varepsilon(\mathbf{k})+i\eta} + \frac{\Theta(k_F-|\mathbf{k}|)}{E-\varepsilon(\mathbf{k})-i\eta} . \tag{2.17}$$

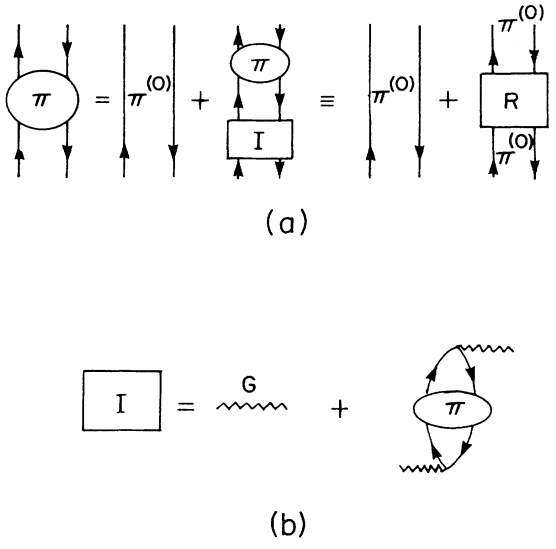

FIG. 2. Nonlinear integral equation relating the *p-h* propagator Π and the irreducible *p-h* interaction *I*. In (a) the first equality gives an RPA-type integral equation for Π. The definition of the reducible *p-h* interaction *R* is also displayed in (a). (b) shows how the irreducible *p-h* interaction *I* depends on the solution Π which leads to the nonlinear structure of the problem. $\Pi^{(0)}$ is the free *p-h* propagator and the wiggly line represents the *G*-matrix interaction. The second term in (b) must be interpreted to include only irreducible contributions to *I*.

The SP spectrum $\varepsilon(\mathbf{k})$ has already been discussed and is given by Eq. (2.3). In the interation process leading to the induced interaction the Landau parameter F_1 changes in each iteration step. This influence on the self-energy is also treated here by changing $\varepsilon(\mathbf{k})$ in each iteration step accordingly. A more-complete calculation should treat the change in the complete self-energy $\Sigma(\mathbf{k},E)$, but this is beyond the scope of the present paper (see also Ref. 30).

With this approximation to the SP propagator in Eq. (2.16) one obtains after performing the ω' integration

$$\Pi^{(0)}(\mathbf{p};\mathbf{q},\omega)=\frac{\Theta(|\mathbf{p}+\mathbf{q}/2|-k_F)\Theta(k_F-|\mathbf{p}-\mathbf{q}/2|)}{\omega-\varepsilon(\mathbf{p}+\mathbf{q}/2)+\varepsilon(\mathbf{p}-\mathbf{q}/2)+i\eta} - \frac{\Theta(|\mathbf{p}-\mathbf{q}/2|-k_F)\Theta(k_F-|\mathbf{p}+\mathbf{q}/2|)}{\omega+\varepsilon(\mathbf{p}-\mathbf{q}/2)-\varepsilon(\mathbf{p}+\mathbf{q}/2)-i\eta}, \tag{2.18}$$

where the first term is associated with a forward propagating *p-h* pair and the second one with backward propagation. The actual numerical calculations are performed for the reducible *p-h* interaction *R* which is graphically defined in Fig. 2. The first iteration step in the solution of the nonlinear scheme of Fig. 2 consists in approximating the irreducible *p-h* interaction *I* by the *G* matrix. This leads to the following integral equation:[31]

$$R^{(1)}(\mathbf{p},\mathbf{p}';\mathbf{q},\omega)=G(\mathbf{p},\mathbf{p}',\mathbf{q})+\int\frac{d^3k}{(2\pi)^3}G(\mathbf{p},\mathbf{k};\mathbf{q})\times\Pi^{(0)}(\mathbf{k};\mathbf{q},\omega)\times R^{(1)}(\mathbf{k},\mathbf{p}';\mathbf{q},\omega)\ . \tag{2.19}$$

Typical diagrams generated by this equation are displayed in Fig. 3. This diagram series is commonly referred to as the bubble series; one must keep in mind, however, that the *G* matrix contains both the direct and exchange contribution. The wiggly line in all the figures represents this *G* matrix with both the direct and the exchange piece.

In the static limit ($\omega=0$) one can obtain the same energy denominator for the forward and the backward propagating part of $\Pi^{(0)}$ by an appropriate change of variables. Using symmetry properties of the interaction one can then show that one can solve Eq. (2.19) directly for the linear combination

$$R^{(1)}_{\pm}(\mathbf{p},\mathbf{p}';\mathbf{q})\equiv\tfrac{1}{2}[R^{(1)}(\mathbf{p}-\tfrac{1}{2}\mathbf{q},\mathbf{p}'-\tfrac{1}{2}\mathbf{q};\mathbf{q}) \pm R^{(1)}(U(\mathbf{p}-\tfrac{1}{2}\mathbf{q}),\mathbf{p}'-\tfrac{1}{2}\mathbf{q};\mathbf{q})]\ . \tag{2.20}$$

The operation *U* is defined by

$$U(\mathbf{p})\equiv U(p,\theta,\phi)=(p,\pi-\theta,\phi)\ . \tag{2.21}$$

With this linear combination, $R^{(1)}_{\pm}$, Eq. (2.19) can be written as

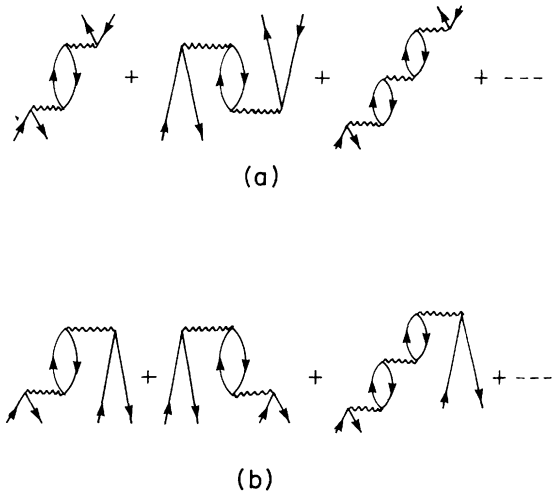

FIG. 3. Typical diagrams which are generated when Eq. (2.19) is iterated with the *G* matrix as the irreducible *p-h* interaction. In (a) the reducible forward-going contributions are given, whereas in (b) the backward-going terms are displayed. It must be kept in mind that in this figure the external lines are not considered as propagators contrary to Fig. 2. Note also that the *G* matrix contains both the direct and the exchange contribution.

$$R_{\pm}^{(1)}(\mathbf{p},\mathbf{p}';\mathbf{q})=G_{\pm}(\mathbf{p},\mathbf{p}';\mathbf{q}) +2\int_X \frac{d^3k}{(2\pi)^3}\frac{G^{\pm}(\mathbf{p},\mathbf{k};\mathbf{q})R_{\pm}^{(1)}(\mathbf{k},\mathbf{q}';\mathbf{q})}{\varepsilon(\mathbf{k})-\varepsilon(\mathbf{k}-\mathbf{q})} . \tag{2.22}$$

The integration area X is determined by

$$0\le k\le k_F , \tag{2.23a}$$

$$-1\le\cos\theta_k\le\min\left[1,\frac{k^2+q^2-k_F^2}{2kq}\right] . \tag{2.23b}$$

The importance of the R_- interacton is intimately connected with the nonlocality of the p-h interaction, here the G matrix. In general, one can show for any interaction operator $\hat{V}$, which depends on the relative distance of the particles only, that the direct p-h matrix element only depends on $\mathbf{q}$ and is in fact the same for the forward [Fig. 4(a)] and the backward contribution [Fig. 4(c)]. For such an interaction only the integral equation for R_+ remains, R_- being identically zero. The exchange terms of $\hat{V}$ bring in the $\mathbf{p},\mathbf{p}'$ dependence, or equivalently make the p-h interaction effectively nonlocal. For the forward contribution shown in Fig. 4(b) the momentum transfer between the particle and the hole is restricted by $2k_F$, since this momentum transfer is absorbed on two hole states. For the backward exchange term [Fig. 4(d)] this restriction does not apply since there the momentum transfer involves a particle and a hole state. From Fig. 4 one can also understand the meaning of U operation [Eq. (2.21)]. It simply corresponds to flipping the initial (or final) p-h state; it transforms diagram (a) to (c) and (b) to (d). One should note, however, that in the latter case a different momentum transfer is involved. This difference is responsible for the appearance of the R_- integral equation and is closely related to the momentum transfer dependence of the interaction in the exchange channel. The P-wave nature of the interaction between spin-aligned ^{3}He atoms implies that this momentum dependence can be strong.

The three-dimensional integral equation (2.22) can be reduced to a set of independent two-dimensional integral equations by employing the fact that the interaction depends only on the difference of the polar angles ϕ_p and $\phi_{p'}$. For more details the reader is referred to Ref. 32.

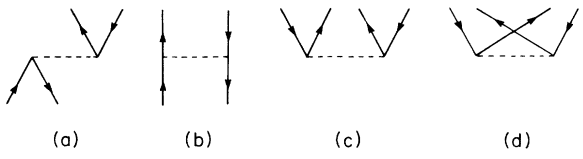

FIG. 4. Different contributions to the p-h interaction from a local interaction $\hat{V}$, e.g., the bare atom-atom potential. (a) represents the forward direct contribution, (b) the forward exchange, (c) the backward direct, and (d) the backward exchange contribution.

According to the scheme depicted in Fig. 2. the induced interaction can now be constructed by calculating the second term on the right-hand side of Fig. 2(b). This step involves attaching four SP propagators to R and inserting this new p-h propagator between the two G matrices. With this new irreducible p-h interaction I one can then go back to the integral equation to construct the new p-h propagator Π and so on until convergence is achieved. This elaborate transformation can be avoided by employing a very reasonable approximation which will now be discussed.

Consider the difference

$$\Delta R^{(1)}(\mathbf{p},\mathbf{p}';\mathbf{q})=R^{(1)}(\mathbf{p},\mathbf{p}',\mathbf{q})-G(\mathbf{p},\mathbf{p}';\mathbf{q}) . \tag{2.24}$$

Here the subscript 1 denotes the first iteration step in the self-consistent determination of the induced interaction [see Eq. (2.19)]. The lowest-order diagram representing this difference is displayed in Fig. 5(a). One observes that this difference may be interpreted as a modification of the direct p-h interaction due to the coupling to the medium. Naturally the diagram in Fig. 5(a) is reducible and should not be used to renormalize the p-h interaction. The corresponding exchange diagram [Fig. 5(b)] is irreducible and in fact the lowest-order contribution to the induced interaction. Instead of using the elaborate construction of I outlined above, we observe that one can obtain diagram 5(b) directly from 5(a) by assuming that the $\Delta R^{(1)}$ interaction depends only on the momentum transfer q. In that case one can treat $\Delta R^{(1)}$ as an operator and simply calculate the exchange part which contributes to the induced interaction. In the actual calculations the additional momentum dependence of ΔR on $\mathbf{p}-\mathbf{p}'$ was taken into account. For more details the reader is referred to Ref. 31.

At this point one can now add the exchange part of $\Delta R^{(1)}$ to the G matrix to obtain the next approximation to the p-h interaction

$$I^{(1)}=G+\Delta R^{(1)}_{\text{exch}} . \tag{2.25}$$

When this interaction is used in Eq. (2.19) one generates, in addition to the original bubble series, diagrams which contain bubbles inside bubbles. A typical example is

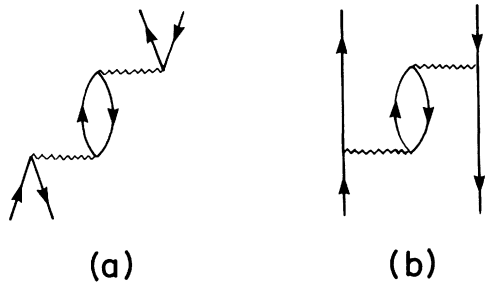

FIG. 5. Lowest-order diagram for the difference ΔR [Eq. (2.24)]. (a) corresponds to the direct contribution which is obtained from Eq. (2.24), the exchange (b) can be obtained by regarding ΔR as an operator and taking the exchange matrix elements (see text).

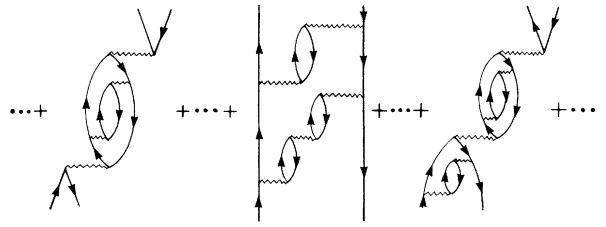

FIG. 6. Typical diagrams which are generated when the first iteration step in the nonlinear scheme of Fig. 2 is included in the *p-h* interaction.

given in Fig. 6. Using Eq. (2.24) for this case, one obtains $\Delta R^{(2)}_{\rm exch}$ which gives a new $I^{(2)}$ and so on. The procedure outlined here can be repeated until self-consistent, at which point the nonlinear scheme of Fig. 2 is solved within the present approximations. It is important to realize that by construction the final solution $I^{(\infty)}$, i.e., the self-consistent one, contains all exchange terms which are generated when $I^{(\infty)}$ is used to solve Eq. (2.19). This ensures that the Pauli principle is automatically fulfilled,[33] and therefore also the sum rule for the Landau parameters [Eq. (2.14)].

As discussed above, we perform the calculation of the induced interaction at $\omega=0$. The construction of the induced interaction disregards the energy dependence of the induced interaction. Although a treatment of this energy dependence is desirable, it represents a substantial increase over the present, already extensive numerical effort and it is therefore not attempted here. A nice feature of the self-consistent scheme is, however, that although the neglect of the energy dependence might lead to a slight overestimate of the induced interaction in the first iteration step, this overestimate will also be counterbalanced by a somewhat too large screening contribution and so on. This will lead to a substantial cancellation, so that one may hope that the neglect of the energy dependence is not too serious.

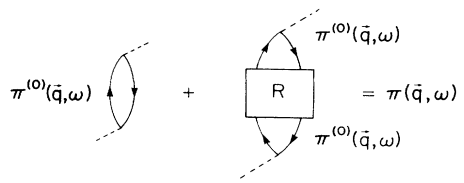

FIG. 7. Contributions to the *p-h* propagator Π, see Eq. (2.26). The first term corresponds to the Lindhard function. The second term includes at least one interaction term. Note that the full reducible interaction R contains all possible screening diagrams and reducible diagrams. The above diagrams should be considered as Feynman diagrams containing both forward and backward propagating contributions.

C. Analysis of the induced interaction

The analysis of the irreducible *p-h* interaction I is somewhat complicated due to the treatment of the full momentum dependence of the interaction. In the Landau limit the interaction can be represented by the Landau parameters F_l, and the influence of the induced interaction on these parameters will be discussed in Sec. III. For finite values of the momentum transfer q one would still like to have a meaningful way of analyzing the interaction. In order to perform this analysis we have calculated from the reducible *p-h* interaction R the Fourier transform of the density-density correlation function[34]

$$\Pi(\mathbf{q},\omega)=\Pi^{(0)}(\mathbf{q},\omega)+\int\frac{d^3p}{(2\pi)^3}\int\frac{d^3p'}{(2\pi)^3}\Pi^{(0)}(\mathbf{p};\mathbf{q},\omega)\times R(\mathbf{p},\mathbf{p}';\mathbf{q},\omega)\times\Pi^{(0)}(\mathbf{p}';\mathbf{q},\omega)\ , \tag{2.26}$$

where $\Pi^{(0)}(\mathbf{q},\omega)$ is the Lindhard function[34] and $\Pi^{(0)}(\mathbf{p};\mathbf{q},\omega)$ is discussed in Sec. II A. Equation (2.26) shows that the full momentum dependence of R is taken into account in the calculation of $\Pi(\mathbf{q},\omega)$. We will restrict ourselves, however, to the static limit $\omega=0$. In this limit the polarization propagator $\Pi(\mathbf{q},\omega=0)$ is purely real since no *p-h* excitations can be created on-shell. For $\omega\neq0$, Π becomes complex and its imaginary part is proportional to the dynamic structure function $S(\mathbf{q},\omega)$.[34] Here we only consider the static limit of Π.

The diagrammatic content of Eq. (2.26) is shown in Fig. 7. The relation between the Lindhard function and $\Pi^{(0)}(\mathbf{p};\mathbf{q},\omega)$ is given by

$$\Pi^{(0)}(\mathbf{q},\omega)=\int\frac{d^3p}{(2\pi)^3}\Pi^{(0)}(\mathbf{p};\mathbf{q},\omega)\ . \tag{2.27}$$

If the irreducible interaction I would only depend on the conserved *p-h* momentum $\mathbf{q}$ one can obtain $\Pi(\mathbf{q},\omega=0)\equiv\Pi(\mathbf{q})$ from the algebraic equation

$$\Pi(\mathbf{q})=\Pi^{(0)}(\mathbf{q})+\Pi^{(0)}(\mathbf{q})I(\mathbf{q})\Pi(\mathbf{q})\ . \tag{2.28}$$

The complete numerical calculation of $\Pi(\mathbf{q})$ according to Eq. (2.26) can now be used to define an average quantity $I(\mathbf{q})$, which is required to give the same numerical result for $\Pi(\mathbf{q})$ but now calculated according to Eq. (2.28). In this analysis there are actually two functions $I^{\pm}$ corresponding to the integral equations for $R^{\pm}$ which were discussed in Sec. II B. The numerical calculation therefore yields two different contributions illustrated graphically in Fig. 8. Equation (2.28) can then be extended to two functions $I_{fw}(\mathbf{q})$ and $I_{bw}(\mathbf{q})$ leading to coupled equations

$$\Pi_{\rm fw}(\mathbf{q})=\tfrac{1}{2}[\Pi^{(0)}(\mathbf{q})+\Pi^{(0)}(\mathbf{q})I_{\rm fw}(\mathbf{q})\Pi_{\rm fw}(\mathbf{q})+\Pi^{(0)}(\mathbf{q})I_{\rm bw}(\mathbf{q})\Pi_{\rm bw}(\mathbf{q})] \tag{2.29}$$

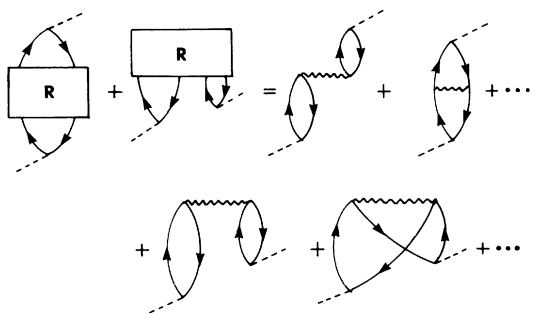

FIG. 8. Illustration of forward and backward contributions to $\Pi(\mathbf{q})$ from the folding of R with $\Pi^{(0)}(\mathbf{p};\mathbf{q})$ and $\Pi^{(0)}(\mathbf{p}';\mathbf{q})$ in Eq. (2.26).

and

$$\Pi_{\rm bw}(\mathbf{q})=\tfrac{1}{2}[\Pi^{(0)}(\mathbf{q})+\Pi^{(0)}(\mathbf{q})I_{\rm bw}(\mathbf{q})\Pi_{\rm fw}(\mathbf{q}) + \Pi^{(0)}(\mathbf{q})I_{\rm fw}(\mathbf{q})\Pi_{\rm bw}(\mathbf{q})] \ . \tag{2.30}$$

When $I_{\rm fw}=I_{\rm bw}$, Eqs. (2.28) and (2.29) reduce to Eq. (2.27). Obviously

$$\Pi(\mathbf{q})=\Pi_{\rm fw}(\mathbf{q})+\Pi_{\rm bw}(\mathbf{q}) \tag{2.31}$$

and it is possible to solve Eqs. (2.29) and (2.30) by requesting that the numerically calculated $\Pi_{\rm fw}(\mathbf{q})$ and $\Pi_{\rm bw}(\mathbf{q})$ are reproduced by $I_{\rm fw}(\mathbf{q})$ and $I_{\rm bw}(\mathbf{q})$. Alternatively, one can consider again the linear combinations

$$I^{\pm}(\mathbf{q})=\tfrac{1}{2}[I_{\rm fw}(\mathbf{q})\pm I_{\rm bw}(\mathbf{q})] \ , \tag{2.32}$$

which brings us back to the discussion of Sec. II B. Solving for $\Pi(\mathbf{q})$, one obtains

$$\Pi(\mathbf{q})=\frac{\Pi^{(0)}(\mathbf{q})}{1-\Pi^{(0)}(\mathbf{q})I^{+}(\mathbf{q})}\equiv\frac{\Pi^{(0)}(\mathbf{q})}{1+X^{+}(\mathbf{q})} \ , \tag{2.33}$$

where $X^{+}(\mathbf{q})$ can be interpreted as a measure of the stability of the ground state with respect to p-h excitations with momentum q. It is also a natural extension of the criterion of stability on the Landau parameter F_0 in the limit $q=0$. When the function $X^{+}(\mathbf{q})$ approaches -1 in a certain momentum range, one is near an instability. Similarly, one can define

$$X^{-}(\mathbf{q})\equiv-\Pi^{(0)}(\mathbf{q})I^{-}(\mathbf{q}) \ . \tag{2.34}$$

Finally, we introduce the "static dielectric" function

$$\varepsilon(\mathbf{q})=1+X^{+}(\mathbf{q}) \ . \tag{2.35}$$

It is even more illustrative to discuss $1/\varepsilon(\mathbf{q})$; this quantity determines whether the total response function $\Pi(\mathbf{q})$ is enhanced (>1) with respect to $\Pi^{(0)}(\mathbf{q})$ or quenched (<1).

III. RESULTS AND DISCUSSION

The calculation of the induced interaction has been performed at two different densities corresponding to the Fermi momenta $k_F=0.9$ and 1.0 Å^{-1}, respectively. The choice for $k_F=0.9$ Å^{-1} was made because it represents a "low-density" situation in which the hole-line expansion is expected to be relevant. The other density corresponds to the saturation density of normal ^{3}He; in addition most calculations reported in the literature have been performed for this density. This, therefore, facilitates the comparison with other calculations.

As discussed in Sec. II A, we have made the standard choice for the SP spectrum which is used in the calculation of the G matrix. It is therefore interesting to make a comparison with a calculation which treats the SP spectrum continuous across k_F. In Fig. 9 we compare the SP spectrum obtained from the Galitskiĭ-Feynman T matrix[13] with the lowest-order Brueckner result for $k_F=1.0$ Å^{-1}. The kink in the spectrum at k_F is not very large and our subsequent use of a continuous spectrum will not be too inconsistent with the Brueckner spectrum. As discussed in Sec. II A one expects that one obtains less attraction with this conventional spectrum and this is confirmed by comparing with the continuous spectrum. In both cases the potential energy of the system is calculated by integrating the SP potential energy over the Fermi sea. From Fig. 9 one can therefore infer that the Galitskiĭ-Feynman approach will give more attraction than the conventional G matrix. Indeed the potential energy per particle for the G matrix is -3.28 K compared with -6.27 K for Ref. 14. This is a large difference, which to a large extent can be attributed to the use of a continuous SP spectrum in the Galitskiĭ-Feynman T matrix. One should, however, keep in mind that this results from a double integration over the Fermi sea. The difference between the Landau parameter F_0 will be much smaller and will be disussed later. In addition, we note that neglecting the center-of-mass ($\mathbf{K}$) dependence as in Ref. 14 by simply setting $|\mathbf{K}|=0$ throughout the whole calculation one obtains -3.87 K potential energy for the G matrix.

Comparing with the binding energies which are obtained with other methods,[6–10] one observes that varia-

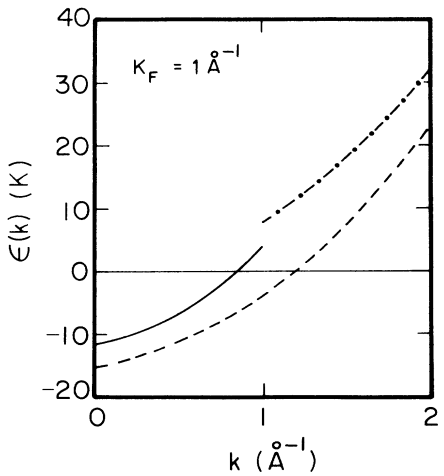

FIG. 9. Comparison of the Galitskiĭ-Feynman SP spectrum (Ref. 14) (dashed line) with the present results for $k_F=1.0$ Å^{-1} solid line for $|\mathbf{k}|<k_F$ and dash-dotted line for $|\mathbf{k}|>k_F$).

tional results and the Galitskiĭ-Feynman T matrix result[14] typically lead to 1 to 2 K binding, instead we obtain 1.54 K repulsion when we add the repulsive kinetic energy contribution to the potential energy. Clearly this is a significant difference. Presumably it can be overcome by an inclusion of three-body correlations as calculated by Day for nuclear matter.[26] Since we are mostly interested in the calculation of the p-h interaction, we think that the use of the G matrix as a starting point for the induced interaction is still a good starting point although probably not the best. The substantial changes in the p-h interaction, which are obtained by including the induced interaction to the G matrix, indicate that a proper inclusion of collective effects is at least as important as fine tuning the treatment of the short-range correlations.

We will begin discussing the results for the p-h interaction in the G matrix approximation and later paying attention to the important changes which occur when the induced interaction is added. In Fig. 10 the results for the Landau parameter F_0 are displayed as a function of the Fermi momentum k_F. The results of the G matrix give an attractive F_0; this is consistent with the results of Ref. 14. A comparison with the direct interaction of Bedell and Quader shows that their starting point for the calculation of the induced interaction is already repulsive and certainly not representative for the G matrix.

In Table I we give the results for the Landau parameters F_l for $l \leq 6$. The results for the G matrix imply that there is a strong indication that higher-order parameters ($l \geq 1$) are not at all negligible. In this context one

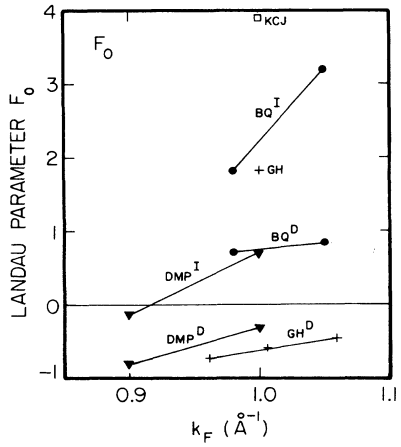

FIG. 10. Comparison of the Landau parameter F_0 as a function of the Fermi momentum for different calculations. The direct interaction of Ref. 11 is denoted by BQ^D, with inclusion of the induced interaction by BQ^I. The results of Ref. 14 are denoted by GH^D, the result obtained by differentiating the energy by GH. The KCJ result is obtained by extrapolating the results of Ref. 17 for the p-h interaction to $|\mathbf{q}| = 0$ and using the appropriate effective mass given in Fig. 9 of that paper. The present G-matrix results are denoted by DMP^D, and the results containing the induced interaction by DMP^I.

TABLE I. Landau parameters for two different densities. The results for $k_F = 0.9$ Å^{-1} are given in the first two columns. The first column contains the results for the G matrix, the second the results with inclusion of the induced interaction. The last two columns corresponds to $k_F = 1.0$ Å^{-1}, with the same order for the G matrix and induced interaction results. The sum rules S_A and S_P in the last two rows correspond to Eqs. (2.15) and (2.14), respectively. The incompressibility β is obtained from Eq. (2.13).

	$k_F = 0.9$ Å^{-1}		$k_F = 1.0$ Å^{-1}	
	G	I	G	I
m^*/m	0.60	0.79	0.48	0.68
F_0	−0.82	−0.15	−0.30	0.70
F_1	−1.19	−0.63	−1.55	−0.95
F_2	0.74	1.63	0.48	1.74
F_3	0.67	−0.01	0.68	0.16
F_4	0.31	0.15	0.36	0.12
F_5	0.13	−0.07	0.16	−0.11
F_6	0.06	0.07	0.08	0.06
S_A	−0.03		−0.03	
S_P	−4.61	0.15	−1.96	0.24
β	1.30	4.66	7.80	13.37

should keep in mind that the p-h interaction is "at least" as complicated as the G matrix. We also note that the Pauli principle sum rule is strongly violated for $k_F = 0.9$ Å^{-1} and somewhat less so for $k_F = 1.0$ Å^{-1}. In Table I we quote results for the sum rules including $l \leq 9$. The sum rule (2.15) is of course fulfilled for the antisymmetrized G matrix. The P wave dominance of the interaction is also illustrated in Figs. 11 and 12, where the Landau function $V(\mathbf{p},\mathbf{p}')$ [see Eq. (2.11)] is plotted for the two different densities as a function of the momentum transfer q_c between p-h states on the Fermi surface. This momentum transfer in the crossed channel is related to the relative p-h momenta in the Landau limit by[32]

$$\mathbf{q}_c = \mathbf{p} - \mathbf{p}' , \tag{3.1}$$

which means that the absolute value is related to the Landau angle $\theta_L \equiv \theta_{\mathbf{p},\mathbf{p}'}$ by the relation

$$\cos\theta_L = 1 - \frac{q_c^2}{2k_F^2} . \tag{3.2}$$

It is clear that an antisymmetrized interaction must vanish at $q_c = 0$ or $\theta_l = 0$ when the lowest L value of the motion is 1 or larger [see Eq. (2.8)]. In addition, there is a strong q_c dependence which is responsible for the large higher-order Landau parameters.

This strong momentum dependence will also be obvious when discussing the p-h interaction away from the Landau limit, i.e., $|\mathbf{q}| > 0$. Before discussing the results for the solution of the RPA integral equation (2.22) it is useful to illustrate that in the case of a one-component fermion system like ^{3}He↑ the momentum dependence in the Landau limit, i.e., on q_c is in a simple way related to the dependence on q, the total p-h momentum when the interaction is local. A local representation of the G matrix has been shown to be quite useful in the nuclear

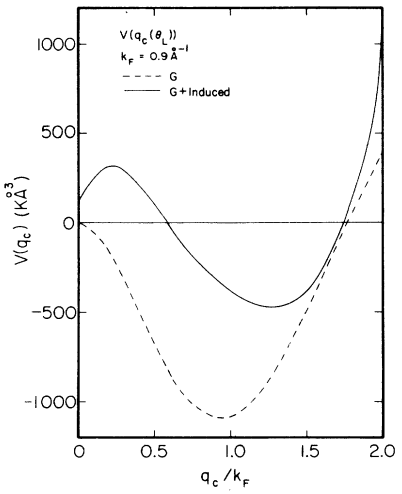

FIG. 11. The p-h interaction V in the Landau limit [see Eq. (2.11)] as a function of the momentum transfer q_c between the p-h states on the Fermi surface as defined in Eq. (3.2) for $k_F=0.9$ Å^{-1}. The dashed line refers to the G-matrix result and the solid line includes the renormalization due to the induced interaction.

case.[35] Assuming a local G matrix operator $g(\mathbf{k})$ which only depends on the momentum transfer $\mathbf{k}$, which is the conjugate momentum of the relative distance of the two atoms, a p-h matrix element acquires a contribution from the direct and the exchange contribution. For the matrix element $G(\mathbf{p},\mathbf{p}';\mathbf{q})$ in Eq. (2.19) one then obtains

$$G(\mathbf{p},\mathbf{p}';\mathbf{q})=g(\mathbf{q})-g(\mathbf{p}-\mathbf{p}'=\mathbf{q}_c)\ . \tag{3.3}$$

This equation shows that the dependence of the interaction on the momentum $\mathbf{q}_c$ in the Landau limit is determined by the same function g which also determines the dependence of the direct part of the interaction on the total momentum $\mathbf{q}$. The solution of the integral equation (2.19) involves matrix elements for one momentum $\mathbf{q}$ and a range of values for $\mathbf{p}-\mathbf{p}'$ (recall the discussion in connection with Fig. 4). Assuming the momentum dependence as displayed in Eq. (3.3), one expects a dependence on $\mathbf{q}$ for the linear combination G_+. In the linear combination G_- this dependence on $\mathbf{q}$ drops out and G_- is dominated by the exchange contribution for which various momenta $\mathbf{p}-\mathbf{p}'$ have to be considered.

We have chosen to show these features by calculating the stability functions $X^+(\mathbf{q})$ and $X^-(\mathbf{q})$ defined in Eqs. (2.33) and (2.34) from the full solution of the integral equations given in Eq. (2.22). We recall that the X^+ can be regarded as a generalization of the Landau parameter F_0 to finite $\mathbf{q}$. The X functions are also dimensionless and contain the proper dependence on the phase space which in the Landau limit is given by N_0. This also allows us to inspect the stability of the ground state with respect to p-h excitations at finite $\mathbf{q}$. Closeness of X to -1 at some $|\mathbf{q}|$ signals such an instability.

In Fig. 13 the $X^{\pm}$ functions are given for $k_F=0.9$ A^{-1} when the G matrix is used in Eq. (2.22) and the resulting reducible p-h interaction is used in Eq. (2.26) to calculate $\Pi(\mathbf{q})$, which in turn can be analyzed according to Eqs. (2.33) and (2.34). As expected, one obtains the dominant q dependence in the X^+ function, but a non-negligible X^- is obtained from the momentum dependence in the exchange contribution. Figure 13 also nicely illustrates the usefulness of the approximate representation of the G matrix given in Eq. (3.3). We know already the expected momentum dependence of the function g from the results of the Landau limit given in Figs. 11 and 12. This implies then according to Eq. (3.3) that X^+ should have an opposite phase as a function of $\mathbf{q}$,

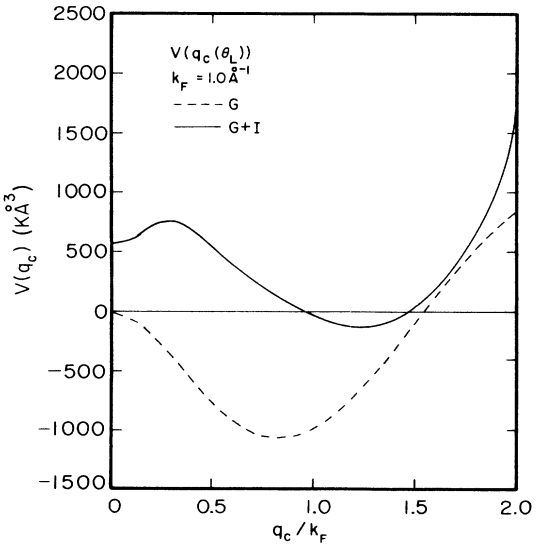

FIG. 12. Same as Fig. 11 for $k_F=1.0$ Å^{-1}.

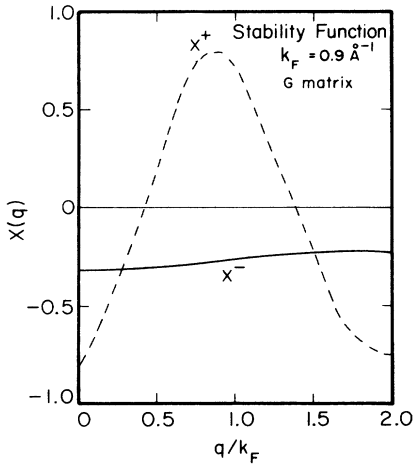

FIG. 13. Stability functions $X^+(\mathbf{q})$ (dashed line) and $X^-(\mathbf{q})$ (solid line) as a function of the total p-h momentum $|\mathbf{q}|$ for $k_F=0.9$ Å^{-1}. These functions are defined in Eqs. (2.33) and (2.34), respectively. The results shown here refer to the G-matrix results at this density.

which in fact is observed in Fig. 13. First there is an increase in X^+ and for momenta $|\mathbf{q}| > k_F$ X^+ is decreasing. The averaging procedure implied in Eq. (2.26) over the momenta $\mathbf{p}$ and $\mathbf{p}'$ is then responsible for an almost $|\mathbf{q}|$ independent shift. This shift is represented in the Landau limit by a simple integral over the angle θ_L and therefore leads to the relation

$$X^+(|\mathbf{q}|=0)=F_0 \ . \tag{3.4}$$

The X^- function is almost $|\mathbf{q}|$ independent if Eq. (3.3) is a reasonable representation of the G matrix, and this is also confirmed in Fig. 13. Since the renormalization due to the induced interaction is more important for the X^+ function, we will focus on this linear combination in the rest of the paper.

For a discussion of the results with inclusion of the fully self-consistently calculated induced interaction we now return to Fig. 10. Comparing our results for the Landau parameter F_0 with the other calculations in the literature a few comments should be made. The first point to raise is the substantially lower value for F_0 we obtain as compared to other calculations. If we compare our values with those of Bedell and Quader[11] at $k_F=1.0$ Å^{-1} we observe that our F_0 is roughly a factor 3 smaller than their value. This implies also a smaller incompressibility (shown in Table I) as compared with the results of Ref. 11. Note that we have drawn a straight line in Fig. 10 to connect the results obtained with the same calculation but for a different density, not implying that this is the actual dependence on the Fermi momentum k_F. As we have discussed above we obtain attractive values for F_0 in the G matrix approximation, whereas in Ref. 11 their direct interaction already gives values which are substantially larger than zero. In addition, they use only the Landau parameters F_0 and F_1 for the direct interaction. More important, however, is that in their scheme the $\mathbf{q}$ dependence of the p-h interaction and therefore the implied $\mathbf{p}-\mathbf{p}'$ dependence on the Fermi surface is not treated adequately. This point can be made clear by considering Fig. 2 again. The irreducible p-h interaction on the Fermi surface, i.e., $|\mathbf{q}|=0$, is constructed by including the phonon exchange which is given by the second term in Fig. 2(b). Even on the Fermi surface these phonons can carry a momentum up to twice the Fermi momentum. In the p-h propagator II in Fig. 2(b) one therefore encounters these larger momenta, and one should then use the appropriate interaction. The p-h interaction in the Landau limit is not a good representation of the p-h interaction at finite q as one can see from Fig. 13, in fact there is a very strong q dependence; it should therefore be no surprise that the calculation of the Landau parameters using only information on the interaction in the Landau limit (the direct interaction in Ref. 11) is not a very good approximation to an inclusion of the full momentum dependence of the interaction, as it is done here. Our results therefore show that one must expect much less repulsive values for the Landau parameter F_0, although the density dependence is similar. This means that F_0 becomes more repulsive at higher density.

In Fig. 10 we have also included the result of Ref. 14 which was obtained by calculating the compressibility from the second derivative of the Galitskiĭ-Feynman energy with respect to the volume. The difference with our result is substantial and much larger than one would expect if one compares the values of F_0 in the G or T matrix approximation. Indeed the more attractive F_0 in the T matrix would lead to a larger renormalization, but this renormalization must also overcome this more attractive original F_0 and the corresponding cancellation effect leads to the expectation that the resulting F_0 cannot be too far away from the corresponding G matrix result. We have therefore no explanation for the large difference, although it must be remarked that it is also unclear in how far this functional differentiation can represent the detailed calculation of the induced density fluctuations as they are reported here.

Finally, we show an extrapolation of the results for the effective p-h interaction calculated with correlated basis functions,[17] to $|\mathbf{q}|=0$. A comparison for the full p-h interaction will be discussed later. In Ref. 17 the local approximation to the p-h interaction[18] was employed. It is therefore likely that this will not be too good an approximation in the Landau limit where the results are strongly influenced by the $|\mathbf{p}-\mathbf{p}'|$ dependence. In addition, one must keep in mind that the approximation we make in the construction of the induced interaction becomes exact in the Landau limit. Here we are referring to the operation discussed in connection with Fig. 5 and Eq. (2.24).

The results for the other Landau parameters with inclusion of the induced interaction are collected in Table I. We observe that there are also substantial modifications of the higher-order parameters. The equivalent results in terms of the function $V(\mathbf{p},\mathbf{p}')$ of Eq. (2.11) are displayed in Figs. 11 and 12 for the two different densities. To understand this renormalization it is useful to include the results for the stability functions with inclusion of the induced interaction in the discussion. These results are displayed in Figs. 14 and 15. The solid curves there give the self-consistent results which in turn help to understand qualitatively the renormalization in the Landau limit as a function of q_c. One should keep in mind again that the exchange term corresponding to the difference $\Delta R^{\{\infty\}}_{\text{exch}}$ [see the discussion under Eq. (2.24)] is responsible for this renormalization. According to Figs. 14 and 15 this renormalization is substantial for momenta below $1.5k_F$ and momenta close to $2k_F$. This explains then the qualitative behavior of the renormalization in the Landau limit, since only when the X^+ function is far from the value zero does one observe deviations from the free Fermi gas Lindhard function. It is therefore clear that around $q_c=1.5$ Å^{-1} there is only a very small renormalization as shown in Figs. 11 and 12.

This behavior of the renormalization in the Landau limit induces apart from a substantial increase in F_0 a very different set of Landau parameters as compared to the G matrix result. For both densities there is a reduction of F_1 leading to an increase of the effective mass. Since we only treat the complete momentum dependence

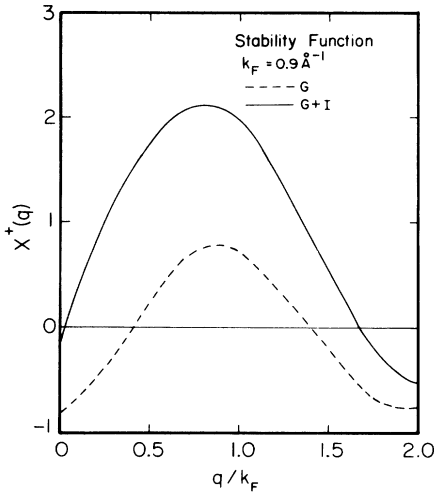

FIG. 14. Same as Fig. 13. The dashed curve here corresponds to the G-matrix results for X^+, the solid line includes the effects of the induced interaction. The Fermi momentum has the value 0.9 Å $^{-1}$.

of the interaction, we can only claim that we include a careful treatment of the so-called k mass.[27] The enhancement at the Fermi surface due to the energy dependence is not included as discussed in Sec. II. We obtain effective masses which are comparable with the results of Ref. 17. However, we cannot present any new information on the discrepancy between the Galitskii-Feynman result[14] for the effective mass and the CBF result[17] as discussed by Mahaux *et al.*[28]

Due to our more complicated interaction we obtain also nonvanishing higher-order Landau parameters. As discussed above we believe that this result is not surprising since we include the effect of the finite $|\mathbf{q}|$ p-h interaction on the irreducible p-h interaction. The result of Bedell and Quader, who observe a rapid convergence with l, is therefore not valid when the induced interaction is calculated on a microscopic level. We also observe that the Pauli principle sum rule [Eq. (2.14)] is fulfilled much better by the Landau parameters which include the effects of the induced interaction, than by those derived from G-matrix approximation. This is not surprising since the present method should preserve this sum rule. We do not obtain exactly zero, however, since the numerical approximations employed do not allow an accurate determination of the Landau parameters for very large l. We have therefore restricted the sum to $l \leq 9$.

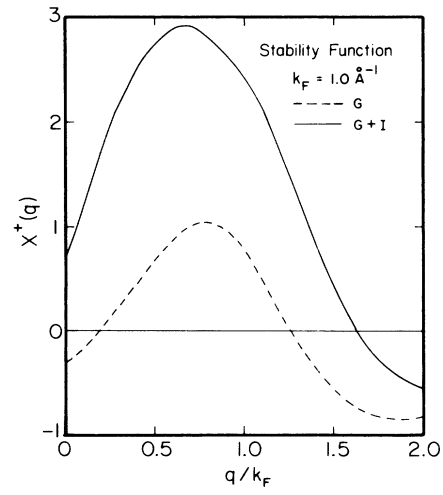

FIG. 15. Same as Fig. 14 for $k_F = 1.0$ Å $^{-1}$.

We now turn to the discussion of the results for the p-h interaction which are obtained for finite values of the p-h momentum $\mathbf{q}$. The results for the stability functions $X^+(\mathbf{q})$ are displayed in Figs. 14 and 15 for $k_F = 0.9$ Å $^{-1}$ and $k_F = 1.0$ Å $^{-1}$, respectively. It is good to remember that the influence of the induced interaction is felt through the exchange term of R^+, it is therefore expected that this influence is represented by a smooth function of $\mathbf{q}$ since the exchange terms are sampled in a way which can only induce a weak $\mathbf{q}$ dependence [e.g., see Eqs. (2.22) and (2.26)]. To understand the sign of the renormalization, one can consider Eq. (2.19) for the case when the p-h interaction depends only on $\mathbf{q}$

$$R(\mathbf{q}) = I(\mathbf{q}) + I(\mathbf{q})\Pi^{(0)}(\mathbf{q})R(\mathbf{q}) \ . \tag{3.5}$$

Here, we have used the static limit ($\omega = 0$) and generalized the p-h interaction to the complete irreducible one, denoted by I. Solving Eq. (3.5) in this simple example, one obtains for the difference $\Delta R = R - I$

$$\Delta R(\mathbf{q}) = \frac{\Pi^{(0)}(\mathbf{q}) I^2(\mathbf{q})}{1 - I(\mathbf{q})\Pi^{(0)}(\mathbf{q})} \ . \tag{3.6}$$

When the stability condition in the denominator is not violated one sees that ΔR is always negative since $\Pi^{(0)}$ is always negative in the static limit. Taking the exchange contribution to obtain the contribution to the irreducible interaction under the assumptions discussed in Sec. II B, one obtains an additional minus sign and therefore the induced interaction gives a repulsive contribution to the p-h interaction. In addition, it is clear from Eq. (3.6) that this contribution is important either when the interaction is sufficiently attractive, where the denominator becomes small, or when the interaction is sufficiently repulsive in which case the denominator becomes comparable with $-I\Pi^{(0)}$ and ΔR is roughly equal to $-I$. Both cases are actually fulfilled on the G-matrix level of approximation as can be seen from the dashed lines in Fig. 14 and 15. This means that it is essential to include the effects of the induced interaction in order to obtain reliable results for the residual p-h interaction. From these simple arguments one can also understand that the induced interaction becomes increasingly important for increasing density. This feature is also observed in the case of nuclear matter[30] where the situation is more complicated due to the presence of more p-h channels and their coupling.

The resulting stability functions are therefore more "stable" (i.e., further away from -1) than the G matrix result. Another important observation is that the effect of the induced interaction becomes substantially less im-

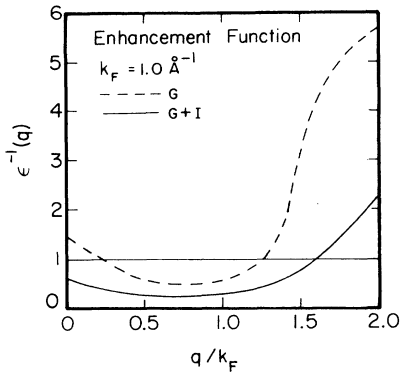

FIG. 16. The inverse of the static dielectric function [Eq. (2.35)], the "enhancement" function, as a function of $|\mathbf{q}|$. This function emphasizes the attractive nature of the interaction and a divergence indicates an instability with respect to p-h excitations with corresponding momentum $|\mathbf{q}|$.

portant for momenta near $2k_F$. This is not surprising because one expects long-range correlations to decrease in magnitude for higher momentum transfers and the short-range correlations which are incorporated in the G matrix to take over. Another useful way of representing the results is depicted in Fig. 16, where the enhancement function $1/\varepsilon(\mathbf{q})$ is shown. The dielectric function $\varepsilon(\mathbf{q})$ is defined in Eq. (2.35). This way of representing the results emphasizes the attractive features of the interaction in particular, and it is clear that the strong enhancement observed for the G matrix is effectively kept under control when the induced interaction is included.

Finally, we plot in Fig. 17 the irreducible p-h interaction $I^+(\mathbf{q})$ as a function of $|\mathbf{q}|$ for the two different densities. Also given in Fig. 17 is the result of Ref. 17 for a density which corresponds to $k_F=0.994$ Å^{-1}. The first observation is the good agreement between the two completely different calculations for momenta larger than $0.5k_F$. This agreement is due to the inclusion of the induced interaction as demonstrated in Figs. 14 and 15. Also, the density dependence of the result for $I^+(\mathbf{q})$ is in complete agreement with the results shown in Fig. 4 of Ref. 17 (not explicitly shown here). The agreement for the p-h interaction calculated by means of completely orthogonal methods therefore strongly reinforces the credibility of both calculations. The remaining discrepancy is nevertheless substantial for small momenta $|\mathbf{q}|$ which leads to large differences in the Landau parameter F_0 (see Fig. 10). As discussed before our results should be most accurate in the Landau limit leading, e.g., to a fulfillment of the Pauli principle sum rule for the Landau parameters. It should therefore be interesting to further explore this difference between both calculations at small momenta where one is more sensitive to the nonlocalities of the interaction which are not explicitly included in the calculation of Ref. 17.

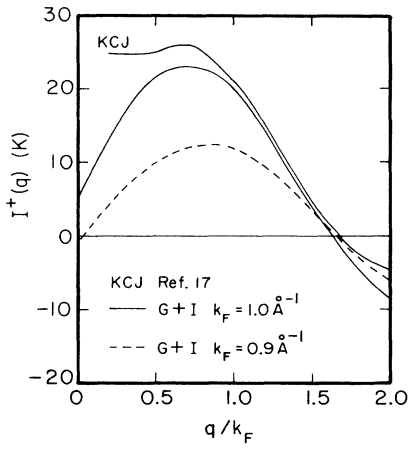

FIG. 17. The results for the irreducible p-h interaction $I^+(\mathbf{q})$ as a function of $|\mathbf{q}|$ for two different densities. The results include the full momentum dependence of the induced interaction and are obtained by analyzing $\Pi(\mathbf{q})$ in terms of Eq. (2.33). The dashed curve refers to $k_F=0.9$ Å^{-1} and the solid line to $k_F=1.0$ Å^{-1}. The solid line labeled KCJ gives the results of Ref. 17 for a density which corresponds to $k_F=0.994$ Å^{-1}. The agreement between the two methods for $|\mathbf{q}|>k_F$ is encouraging.

IV. CONCLUSIONS AND SUMMARY

In this paper a microscopic investigation of the residual p-h interaction in fully polarized liquid helium is reported. The method is based on the concept of the induced interaction which (self-)consistently includes the phonon exchange terms into the residual p-h interaction. The starting point of the calculation is the Brueckner G matrix which takes care of the short-range correlations between the atoms. The continuous choice for the SP spectrum in the Galitskiĭ-Feynman T matrix[14] leads to a substantially lower energy as compared with our G- matrix results which are calculated with a gap in the SP spectrum. For the p-h interaction as exemplified by the Landau parameter F_0, we obtain a similar result as in Ref. 14. We observe that the direct interaction of Bedell and Quader[11] is not representative of such a microscopic interaction.

A study of the p-h interaction including the full momentum dependence of the interaction, reveals that the nonlocality of the p-h interaction is non-negligible. The inclusion of this momentum dependence in the induced interaction leads to important renormalization effects on the Landau parameters. Apart from less repulsive values for F_0 as compared with the results of Ref. 11, we also obtain nonvanishing parameters for $l\geq 2$. With this microscopic version of the induced interaction we therefore obtain quite different results than in Ref. 11.

An additional advantage of treating the full momentum dependence of the interaction is the possibility of studying the p-h interaction also for finite values of the momentum transfer $|\mathbf{q}|$. We have analyzed the result of our calculations in terms of stability functions $X(\mathbf{q})$ which measure the closeness of the system to an instabil-

ity of the system with respect to p-h excitations at momentum $|\mathbf{q}|$. The results show that the induced interaction tends to stabilize the system making the p-h interaction more repulsive. Furthermore, it has been shown in terms of a simple model how one can understand the main features of the results. This also illustrates that the inclusion of the induced interaction is essential to obtain reliable results for the p-h interaction. In the Landau limit this is demonstrated by fulfilling the Pauli principle sum rule for the Landau parameters. A comparison with CBF results[17] for the p-h interaction shows encouraging agreement for $|\mathbf{q}| > 0.5k_F$. For the Landau parameter F_0 the CBF yields a considerably larger value.

ACKNOWLEDGMENTS

This research was supported in part by the Condensed Matter Theory Program of the Division of Materials Research of the U.S. National Science Foundation under Grant No. DMR-8519077 (at Washington University) and in part by the Deutsche Forschungsgemeinschaft (DFG, Federal Republic of Germany) and by CAYCIT Grant No. 85-0072-C02-00 (Spain).

[1]B. Castaing and P. Noziéres, J. Phys. (Paris) **40**, 257 (1979).
[2]G. Bonfait, L. Puech, A. S. Greenberg, G. Eska, B. Castaing, and D. Thoulouze, Phys. Rev. Lett. **53**, 1092 (1984).
[3]A. Dutta and C. N. Archie, Phys. Rev. Lett. **55**, 319 (1985).
[4]M. Leduc, P. J. Nacher, S. B. Crampton, and F. Laloë, in *Quantum Fluids and Solids, Sanibel, Florida, 1983,* Proceedings of the Symposium on Quantum Fluids and Solids, AIP Conf. Proc. No. 103, edited by E. D. Adams and G. G. Ihas (AIP, New York, 1983), p. 179.
[5]C. Lhuillier and F. Laloë, J. Phys. (Paris) **40**, 239 (1979).
[6]D. Levesque and C. Lhuillier, J. Phys. (Paris) Colloq. **41**, C7-191 (1980); C. Lhuillier and D. Levesque, Phys. Rev. B **23**, 2203 (1981).
[7]J. W. Clark, E. Krotscheck, and R. M. Panoff, J. Phys. (Paris) Colloq. **41**, C7-197 (1980); E. Krotscheck, R. A. Smith, J. W. Clark, and R. M. Panoff, Phys. Rev. B **24**, 6383 (1981).
[8]K. E. Kürten and C. E. Campbell, J. Low Temp. Phys. **44**, 149 (1981).
[9]J. C. Owen and G. Ripka, Phys. Rev. B **25**, 4914 (1982).
[10]E. Manousakis, S. Fantoni, V. R. Pandharipande, and Q. N. Usmani, Phys. Rev. B **28**, 3770 (1983).
[11]K. S. Bedell and K. F. Quader, Phys. Lett. **96A**, 91 (1983).
[12]T. L. Ainsworth, K. S. Bedell, G. E. Brown, and K. F. Quader, J. Low Temp. Phys. **50**, 319 (1983).
[13]S. Babu and G. E. Brown, Ann. Phys. (N. Y.) **78**, 1 (1973).
[14]H. R. Glyde and S. I. Hernadi, Phys. Rev. B **29**, 3873 (1984).
[15]H. R. Glyde and S. I. Hernadi, Phys. Rev. B **28**, 141 (1983).
[16]H. R. Glyde and S. I. Hernadi, Phys. Rev. B **29**, 4926 (1984).
[17]E. Krotscheck, J. W. Clark, and A. D. Jackson, Phys. Rev. B **28**, 5088 (1983).
[18]E. Krotscheck, Phys. Rev. A **26**, 3536 (1977).
[19]R. A. Aziz, V. P. S. Nain, J. C. Carly, W. J. Taylor, and G. T. McConville, J. Chem. Phys. **70**, 4330 (1979).
[20]I. Ia. Pomeranchuk, Zh. Eksp. Teor. Fiz. **35**, 524 (1958) [Sov. Phys.—JETP **8**, 361 (1959)].
[21]R. M. Panoff, in *Condensed Matter Theories, Vol. 2,* (Plenum, New York, in press).
[22]S.-O. Bäckman, Nucl. Phys. B **130**, 427 (1969).
[23]W. H. Dickhoff, A. Faessler, J. Meyer-ter-Vehn, and H. Müther, Phys. Rev. C **23**, 1154 (1981).
[24]C. H. Aldrich III and D. Pines, J. Low Temp. Phys. **32**, 689 (1978).
[25]D. Pines, in *Recent Progress in Many Body Theories,* Vol. 142 of *Lecture Notes in Physics,* edited by J. G. Zabolitzky, M. de Llano, M. Fortes, and J. W. Clark (Springer, New York, 1971), p. 205.
[26]B. D. Day, Phys. Rev. C **24**, 1203 (1981).
[27]J. P. Jeukenne, A. Lejeune, and C. Mahaux, Phys. Rep. C **25**, 83 (1976).
[28]C. Mahaux, P. F. Bortignon, R. A. Broglia, and C. H. Dasso, Phys. Rep. C **120**, 1 (1985).
[29]S. S. Wu, Sci. Sin. **16**, 347 (1973); **17**, 468 (1984).
[30]W. H. Dickhoff and H. Müther, Nucl. Phys. A (to be published).
[31]W. H. Dickhoff, A. Faessler, H. Müther, and S. S. Wu, Nucl. Phys. **A405**, 534 (1983).
[32]W. H. Dickhoff, A. Faessler, J. Meyer-ter-Vehn, and H. Müther, Nucl. Phys. **A368**, 445 (1981).
[33]W. H. Dickhoff, Prog. Part Nucl. Phys. **12**, 529 (1984).
[34]A. L. Fetter and J. D. Walecka, *Quantum Theory of Many-Particle Systems* (McGraw-Hill, New York, 1971).
[35]W. H. Dickhoff, Nucl. Phys. **A399**, 287 (1983).